Terr. Atmos. Ocean. Sci., Vol. 32, No. 5, Part I, 619-632, October 2021 doi: 10.3319/TAO.2021.07.12.02

A study of the rainfall and structural changes of Typhoon Koppu (2015) over northern Philippines

Tien-Chiang Yeh[1, *], Esperanza O. Cayanan[2], Ling-Feng Hsiao[1], Der-Song Chen[1], and Ya-Ting Tsai[1]

[1] *Central Weather Bureau, Taipei City, Taiwan*
[2] *Department of Science and Technology, Philippine Atmospheric Geophysical and Astronomical Services Administration, Metro Manila, Philippine*

Article history:
Received 22 December 2020
Revised 21 June 2021
Accepted 12 July 2021

Keywords:
Tropical cyclone rainfall prediction, Terrain effect, Philippines, TWRF (Typhoon WRF)

Citation:
Yeh, T.-C., E. O. Cayanan, L.-F. Hsiao, D.-S. Chen, and Y.-T. Tsai, 2021: A study of the rainfall and structural changes of Typhoon Koppu (2015) over northern Philippines. Terr. Atmos. Ocean. Sci., 32, 619-632, doi: 10.3319/TAO.2021.07.12.02

ABSTRACT

Typhoon (TY) Koppu (2015) brought intensive small horizontal-scale rainfall at Baguio, Philippines. This study examines the applicability of the TWRF model (based on the Weather Research and Forecasting model, https://www.mmm.ucar.edu/weather-research-and-forecasting-model, specifically for the TY prediction) of the Central Weather Bureau, Taiwan in the rainfall prediction of Koppu. Moreover, it aims to improve the understanding of the mountainous terrain effect on the rainfall and structural changes of TY Koppu. The TWRF-predicted rainfall initiated at 1200 UTC 17 October is compared with the surface observed rainfall and the passive microwave rainfall product, and the TWRF-simulated TY Koppu structure is verified against satellite infrared cloud imagery. Verifying available best tracks, the largest predicted track error within 72 hours of prediction is 145 km. Rainfall similar to that at Baguio can also be obtained by the TWRF, except that the location of the maximum rainfall is to the south of the observation. Modeling results show that heavy rainfall was caused by the outer rain band of TY Koppu, which gradually reorganized over the western coastal area when Koppu weakened after landing. Results also show that the high terrain located south of the TY center enhanced the rain band. However, the dry air in the lee side and downstream of the high mountains located north of the TY center weakened and pushed the band southward. TY Koppu and the rain band then moved northward. The formation and intensification, the weakening and southward shifting, and then the northward approaching and passing of the rain band resulted in the extreme rainfall at Baguio.

1. INTRODUCTION

The Northwest Pacific has the most number of tropical cyclones (TCs) among the regions, and the Philippines is the most frequently attacked country. Strong typhoons (TYs) are also more concentrated in the east coasts of Taiwan and the Philippines. With high and complex mountainous terrain, the forecast of TCs has been paid exceptional attention to for a long time in Taiwan and the Philippines. Hsu (1960) and Li (1963) listed the difficulties of TC forecast, including that TCs may form subcenters when they encounter Taiwan. Brand and Blelloch (1973, 1974) analyzed the characteristics of TCs crossing the Philippines and Taiwan. They reported that topography changes the size, strength, and movement of TCs. Wang (1980) documented the influence of the mountainous Taiwan terrain on the structure and path changes of TCs affected Taiwan. Wu and Kuo (1999) summarized decades of studies on the understanding of the characteristics of TCs making landfall at Taiwan. The development of numerical forecasting systems (Hong et al. 2015; Hsiao et al. 2020), the application of new observing equipment, such as meteorological satellites and radars (Lee et al. 2000; Liu et al. 2001; Huang et al. 2005), and the observations and research programs (e.g., Lee et al. 2000, 2008; Liu et al. 2001; Huang et al. 2005; Lin et al. 2005; Wu et al. 2007; Chien and Kuo 2011; Wang et al. 2013; Chen et al. 2017; Yang et al. 2018) have contributed to the improvement of the understanding and forecast of the movement and structural changes of TCs in Taiwan.

* *Corresponding author*
E-mail: tcyehcwb@gmail.com

As for TCs in the Philippines, Cayanan et al. (2011) indicated that approximately 19 - 20 TCs enter the Philippine Area of Responsibility every year, with an average of nine TCs making landfall (Cinco et al. 2016). Brand and Blelloch (1973) reported an increase in speed of movement as TCs approach the Philippines. A northward perturbation and an average intensity decrease of 33% were reported as the TCs pass through the Philippines. They also found a decrease in circulation size for weak TCs. Recently, Lin and Chou (2018) reported that the numbers of size increase and size decrease cases are similar for TCs passing through the Philippines. As for the inner core of the TCs, Chou et al. (2011) reported that the radius of the eyewall expands for 87% of landfall TCs during landfall, and it contracts for 57% of the cases when the cyclones re-enter the ocean after crossing the Philippines. An eyewall evolution of TY Zeb (1998) was documented by Wu et al. (2003).

Cinco et al. (2016) showed that TCs contribute approximately 35% to the total annual rainfall for Philippines. One of the peculiar characteristics of TC rainfall in the Philippines was reported by Cayanan et al. (2011). They found cases of indirect TC heavy rainfall when the cyclone moved northeast of Luzon. Heavy rainfall events are caused by the interaction of TCs and southwesterly wind during the boreal summer monsoon period. As for the risk of TCs, Cinco et al. (2016) showed that the estimated normalized cost in damages has a consistently increasing trend. Despite the importance and uniqueness of high terrain in the Philippines, literature on the analysis or forecast of TCs in the area is limited. Thus, further case studies must be conducted to enhance the understanding and improve the forecast of TCs in the region.

In 2015, TY Koppu left a total of 58 deaths, and more than 3 million people were affected. The total estimated cost of damage to agriculture and infrastructure amounted to more than US$ 280 million. This study aims for an improved understanding of the numerical model prediction of TY Koppu, particularly its rainfall and structural changes under the unique high terrain. The TWRF (Hsiao et al. 2020) model established by the Central Weather Bureau (CWB) is applied. In the second section, the TWRF model and TY Koppu (2015) are introduced. Results and discussions on the prediction of the TWRF model on Koppu are provided in the third and fourth sections, respectively. A summary of the study and concluding remarks are presented in the last section.

2. TWRF MODEL, PHILIPPINE TOPOGRAPHY, AND TYPHOON KOPPU

CWB has constructed a regional to mesoscale operational numerical weather prediction system based on the ARW WRF model (https://www.mmm.ucar.edu/weather-research-and-forecasting-model; Skamarock et al. 2008). A development specifically designed for typhoon prediction, the TWRF (Typhoon WRF) model was first operational in 2010 (Hsiao et al. 2010). A version of a two-mesh higher resolution in the 15/3 km model has been used (Hsiao et al. 2020). The initial conditions for the TWRF meshes were provided by the WRF 3DEnVAR, which was embedded in a partial cycling framework consisting of a cold start from the Global Forecast System in National Centers for Environmental Prediction USA (NCEP GFS) analysis 12 h before the initial time, followed by two 6 h assimilation cycles.

The domain of the outer mesh of TWRF applied in this study is the same as in Hsiao et al. (2020). For better coveraging the northern Philippines, the lateral boundary of the inner mesh is extended southward to near 10°N. Inside the inner mesh domain, high mountain ranges are distributed, particularly in Luzon (domain and model terrain height shown in Fig. 1). The Caraballo Mountain Range (CBMR) divides the Luzon Island into Northern Luzon and Central Luzon. The Sierra Madre Mountain Range (SMR) extends on the east side, and the Cordillera Mountain Range (COMR) and the Zambales Mountain Range (ZMR) are located on the west side. Between the mountain ranges are the Cagayan Valley in Northern Luzon and the Central Luzon Plain in Central Luzon. A mountain range also exists in the Mindoro Island, and many high mountain peaks are located in the Bicol Peninsula of Southern Luzon. The distribution of the mountain ranges, valleys, and Philippine cities within the TWRF inner mash are also shown in Fig. 1. The larger-scale mountain ranges have been resolved relatively well in the model. However, small horizontal-scale mountain peaks, such as volcanic mountains in the Bicol Peninsula, are not well resolved by the 3 km resolution grids. The 2463 m peak of the Mayon Volcano was remarkably reduced to less than 1250 meters in the model.

TC Koppu formed as a named tropical storm near 15.8°N, 139.2°E at 1800 UTC 13 October (hereafter denoted as 18 UTC 13, omits October and the 00 after the UTC hour for simplicity). According to the CWB, track in Fig. 1, TC Koppu gradually intensified to a TY at 00 UTC 16 as it moved westward heading toward Northern Luzon, and reached its maximum intensity as a super TY before making landfall on the east coast of Northern Luzon. The TY center deflected northward after making landfall, and gradually weakened to a tropical storm at 00 UTC 19 after the center passed through Luzon. TC Koppu then moved slowly northward along the western coast of Luzon before it recurved to the east at 00 UTC 20, and downgraded to a tropical depression at 18 UTC 20. Strong winds and heavy rainfall were reported over Northern and Central Luzon during the influence of TY Koppu. For examples, 70 and 60 m s^{-1} winds were recorded at Casiguran and Baler, respectively, and 775.4 mm rainfall (170% of the monthly rainfall) was reported at Baguio within a 24-hour period.

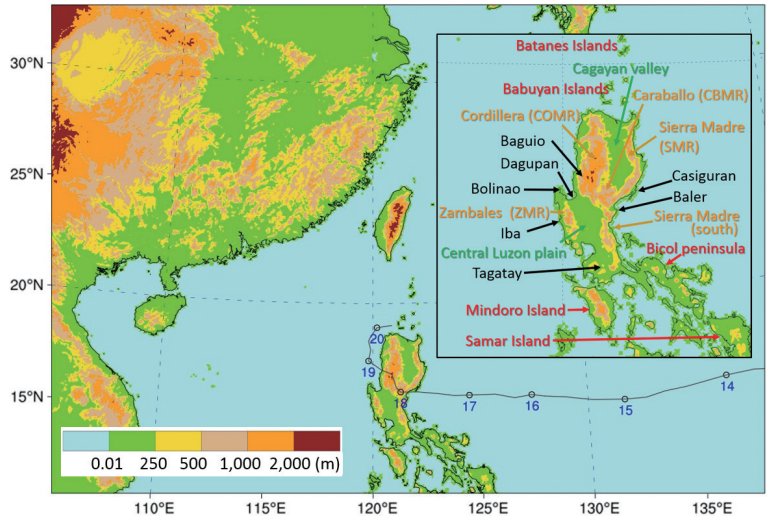

Fig. 1. The domain with the terrain height (shaded, scale in lower-left) of the TWRF model inner mesh, and the best track (center locations at 0000 UTC are marked with date number) of TY Koppu (2015) analyzed by the Central Weather Bureau. Detail distribution of the mountain ranges (name in brown), islands (in red), valleys (in green), and cities (in black) of northern Philippines is shown in the inset.

3. MODEL PREDICTIONS

3.1 Track Prediction

Initiating at 12 UTC 17, the TWRF 72-hour predicted track of TY Koppu is displayed in Fig. 2. The best tracks of TY Koppu observed by the Japan Meteorological Agency (JMA), by the Join Typhoon Warning Center, US (JTWC), and by the Philippine Atmospheric, Geophysical, Astronomical Services Administration (PAGASA) are also displayed in the figure. Verifying all best tracks, the largest TWRF-predicted track error within 72 hours of prediction is 145 km that occurred at 60 hours of prediction. The major error occurred as the TWRF predicted the system moving more westward, whereas some observed Koppu drifting northward in central Northern Luzon after 00 UTC 18. A similar westward movement of the TY to cross the Luzon Island was reported by the JTWC. The error is 77/137/100/122/107 km for 24/36/48/60/72 hours of prediction. Very similar location of the TY centers was analyzed by the operational agencies before the centers made landfall. The difference was evident and grew with time after the center moved over land. The uncertainty of the center location grew as the center of the weakened TY was unclear from the satellite imagery, and no other observations, such as those from radar or surface stations, was available.

3.2 Rainfall Prediction

Four continuous periods of the observed and TWRF-predicted 12-hour accumulated rainfall from 12 UTC 17 to 12 UTC 19 are given in Fig. 3. The surface rainfall observation stations of PAGASA are not well covered in a fine scale at the time TY Koppu made landfall at the Philippines. The average distance between stations is approximately 100 km, and the stations are mainly distributed along the coastal area. To facilitate the rainfall analysis and prediction verification, the analyzed rainfall by the NOAA CPC using the morphing technique (Joyce et al. 2004, http://www.cpc.ncep.noaa.gov/products/janowiak/cmorph_description.html, hereafter referred to as CMORPH rainfall) are also provided in the figure. By including satellite observational information, the CMORPH rainfall could estimate the rainfall over ocean to show the rainfall distribution of the entire TY system. There were roughly four stages of TY Koppu movement during the period from 12 UTC 17 to 12 UTC 19: Moved for landfall (Stage I, from 12 UTC 17 to 00 UTC 18), moved over land (Stage II, from 00 UTC to 12 UTC 18), moved to the ocean (Stage III, from 12 UTC 18 to 00 UTC 19), and moved further northward (Stage IV, from 00 UTC to 12 UTC 19). A similar westward shift from Stage I to Stage II and northward shift from Stage II to Stage III of the heavy rainfall area were found from the observed and CMORPH rainfall. Differences between the observed rainfall and CMORPH rainfall lie in the magnitude of rainfall amount and the detailed distribution of rainfall.

In Stage I (Fig. 3a), the maximum rainfall of 212 mm was measured near the TY center's landing site at Casiguran, and less than 30 mm rain was observed over Western Luzon. However, rainfall of larger than 300 mm, and much larger area with rain greater than 70 mm were found from CMORPH analysis. In Stage II (Fig. 3b), the maximum observed rain was reduced to 113 mm. The CMORPH rainfall shows a similar trend of rainfall decrease. Rain larger than 130 mm was observed over the southern portion of

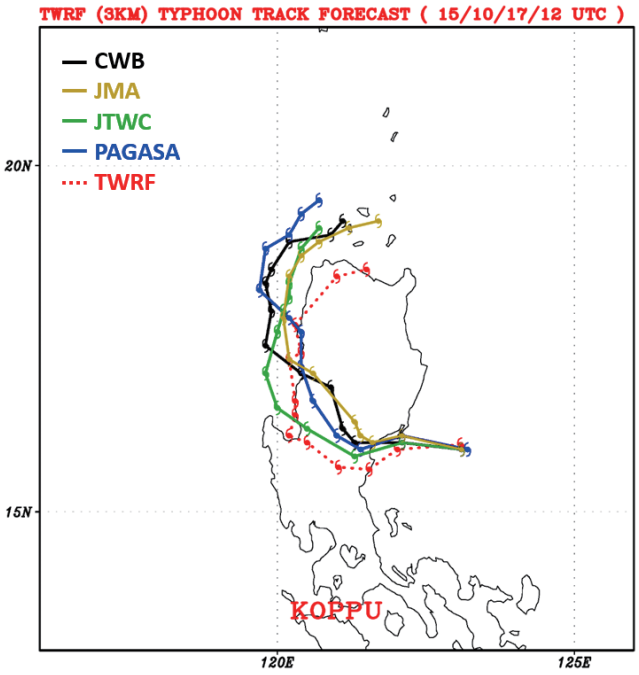

Fig. 2. TWRF's 72-hour forecast track (in red) for TY Koppu initiated at 12 UTC 17 October and the best tracks of the Central Weather Bureau (CWB), Japan Meteorological Agency (JMA), Joint Typhoon Warning Center/USA (JTWC), and PAGASA, for the same period. Symbols in 6-hour intervals.

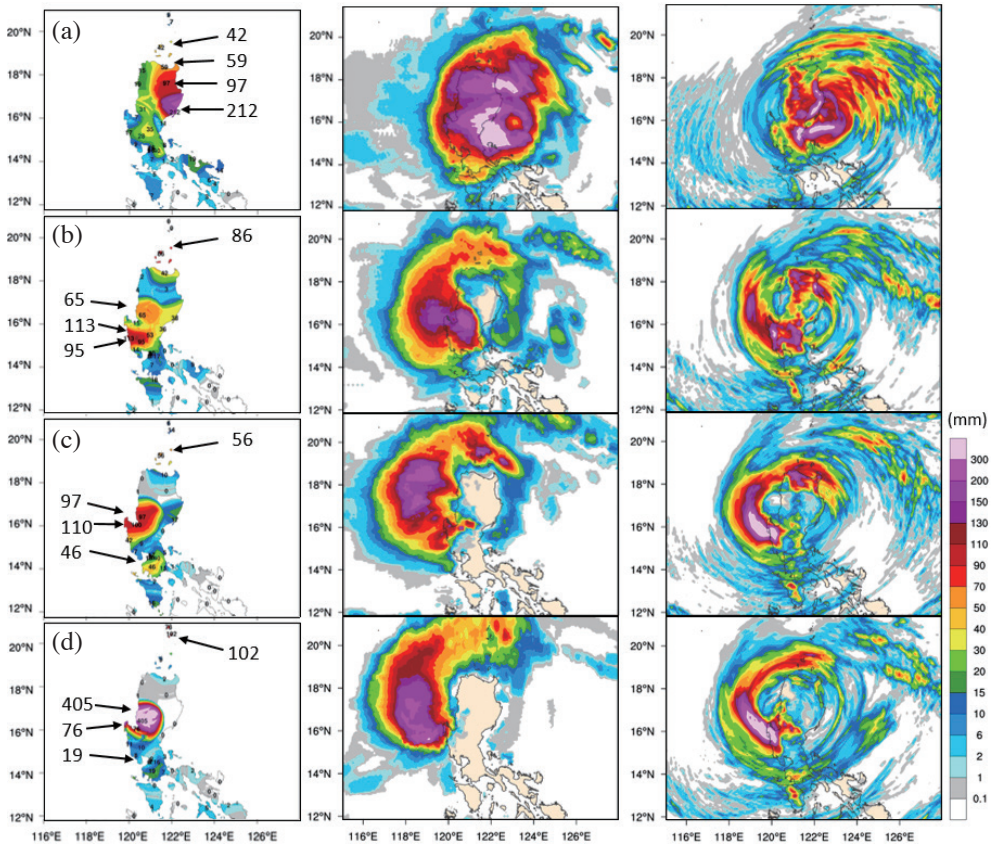

Fig. 3. Twelve-hour accumulated rainfall (mm) observed by the PAGASA surface station (left panel), from the CMORPH analyses (middle), and TWRF prediction (right) at (a) 00 UTC 18 (Stage I, see text), (b) 12 UTC 18 (Stage II), (c) 00 UTC 19 (Stage IIII), and (d) 12 UTC 19 October (Stage IV).

the COMR. Larger rainfall also extended to the west and extended circularly further to the Bashi Channel. The appearance of the rainfall distribution resembled a typical TY rain band. The measured rainfall of 88 mm in Babuyan Island, and the rainfall in Babuyan persisted to the next stage (56 mm in Fig. 3c) before moving northward to the Batanes Island at Stage IV (102 mm in Fig. 3d), verifying the existence and the gradual northward shift of the rain band over the Bashi Channel. For Stages III and IV (Figs. 3c and d), the maximum observed rainfall maintained at approximately 110 mm before 00 UTC 19 and considerably enhanced to 405 mm later. The CMORPH rainfall shows that the rainfall over Luzon was restricted to a small area near Bolinao. After 12 UTC 19, the CMORPH rainfall area (figures not shown) moved off from the land to the ocean. The CMORPH rainfall could show the general rainfall distribution of the TY system, but it could not correctly reflect the detailed rainfall distribution of TY Koppu over Luzon.

Similar to the distribution of CMORPH rainfall, the rainfall predicted by TWRF (Fig. 3) showed an area with rainfall greater than 300 mm in Stage I. Heavy rainfall not only occurred near the center's landfall area but also extended southwest, along the upwind side of the SMR. Strong rain belts were also observed in nearby oceans east of Northern Luzon. However, the TWRF-predicted rainfall over the Cagayan Valley, Western Luzon, and the Central Luzon Plain was much smaller than the CMORPH rainfall and was more similar to the observed rainfall values. The TWRF also predicted that the major rainfall area shifted from eastern Luzon to Western Luzon from Stage I to Stage II, and a rain band formed over central Luzon, extending to the nearby ocean in Stage II. When the observed area of the rainfall maximum shifted from south to north during Stages III and IV, both the TWRF predicted area of the rainfall maximum and the CMORPH analyzed area of the rainfall maximum remained at about the same location near Bolinao. However, similar to the observation, very intensive rainfall was predicted over land. For the later stages of prediction after 12 UTC 19 (Fig. 4), TY Koppu gradually moved northward and then turned northeastward before weakening to a tropical depression. The observed rainfall in Western Luzon remained at the similar location and similar intensity at 00 UTC 20, considerably decreased at 12 UTC 20, and slightly increased and gradually shifted northward at 00 UTC 21. The maximum observed rainfall value decreased to 33 mm at locations near the northwestern corner of Luzon at 12 UTC 21. A similar intensive and small-scale rain band and a similar trend of the shifting of the rain band were predicted by TWRF. However, a considerable rainfall reintensification predicted at 72 h (12 UTC 20) was different from the observation, and the rainfall intensities were also over predicted at 00 UTC 21.

4. DISCUSSION

4.1 Rainfall and Formation of Rain Band

The TWRF-predicted rainfall sequence from 12 UTC 19 to 12 UTC 20 (Fig. 4) shows that the rainfall amount decreases during the first 12 hours before regaining intensity as the rain system contracts to a smaller size and more intensive band. A similar phenomenon is revealed in the 3-hour accumulated rainfall measured at the Baguio station (Fig. 5). The figure indicates that the rain at Baguio is composed of two waves of intensive rain exceeding 100 mm/3 h. The TWRF-predicted rainfall sequence in Baguio also exhibits two similar picks of heavy rain, but the timing is delayed and the amount is smaller. Given that Baguio is where the heaviest rainfall was observed, a location (120.0°E,

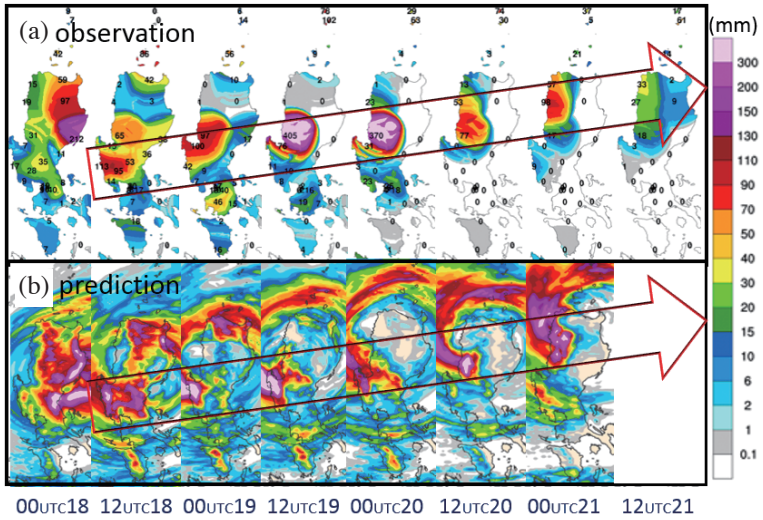

Fig. 4. Sequences of the 12-hour accumulated rainfall observed by PAGASA (upper panel) and the TWRF model prediction (bottom panel) from 00 UTC 18 to 12 UTC 21 October (prediction to 00 UTC 21 October). The arrows show the gradual shifting of the major rainfall area.

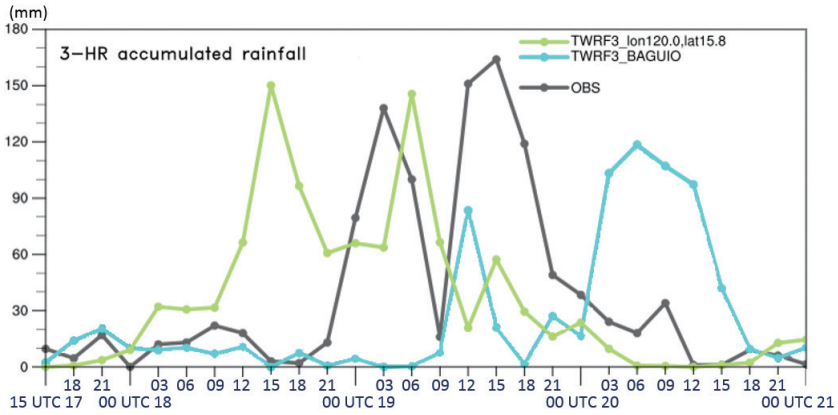

Fig. 5. Sequence of the 3-hour accumulated rainfall (vertical axis, in mm) at Baguio observed by PAGASA (black) and TWRF model prediction (light blue) from 15 UTC 17 to 00 UTC 21 October (from left to right). The TWRF model predicted 3-hour accumulated rainfall at a selected location (15.8°N, 120.0°E), i.e., where the highest accumulated rainfall is predicted in the Philippines, is plotted in light green.

15.8°N) where the highest accumulated rainfall is predicted by the TWRF is selected to represent the model-predicted rainfall at Baguio. The sequence of the predicted 3-hour accumulated rainfall at this selected location (Fig. 5) shows similar amount of rainfall extreme and similar two waves of intensive rain as observations are predicted. However, the time of the intensive rains at the selected location is 9 - 12 hours earlier than that at Baguio.

No complete radar observation was obtained because PAGASA's weather radar in Baler was damaged by TY Koppu. Sequence of diagrams of the multifunctional transport satellite (MTSAT) infrared (IR) imagery as well as TWRF-predicted 10 m winds and radar reflectivity are displayed in Fig. 6 to validate model prediction and to explore the change of TY structure and cloud band distribution when Koppu passing through Luzon. At 12 UTC 17 (inset in left panel of Fig. 6a), the MTSAT cloud top temperature (hereafter CCT) imagery shows that Koppu was intense and well organized with a clearly visible eye and the eye wall of CCT lower than 80°C (hereafter CCT80) circling around the center. In the next 18 hours (Figs. 6a - c), the area of CCT80 shrank with time indicating Koppu weakened gradually as it moving westward along 18°N. The CCT80 limited to a tiny area in Central Luzon with the eye invisible at 06 UTC 18 (Fig. 6c). Higher developing clouds located more in the west side of the system. Away from the TY center, Figs. 6a to c show that the mountainous area in north of the center had a higher developing cloud band, and the band shifted northward. Later, the cloud over Northern Luzon reintensified at 12 UTC 18 (Fig. 6d) and moved northward at 18 UTC 18 (Fig. 6e). The cloud over the ocean west of Luzon (Area A) also developed but shifted southward. Meanwhile, the cloud development near Koppu's center reached to a minimum at 12 UTC 18 (Fig. 6d) before re-intensified and shifted slightly northward at 18 UTC 18 (Fig. 6e).

Similar scenario of cloud development and structural change of TY Koppu is simulated by TWRF (right panel of Fig. 6). At the initial stage of model prediction (inset in right panel of Fig. 6a), the simulated TY was also intense and well organized with clearly visible eye and eye wall. Six hours later, the simulated TY eye changed to an elliptical shape with eye wall reflectivity reduced, and the wind speed decreased. The simulated TY weakened even more in the next 18 hours. The area of stronger echoes (reflectivity higher than 35 dBz, hereafter denoted as higher dBz) area shrank. At 06 UTC 18 (Fig. 6c), higher dBz area limited at the southwest quadrant of the TY circulation near center. A large portion of the simulated TY, particularly in westside and northside, is echo free. As TY moving further inland at 12 UTC 18 (Fig. 6d), the echo free area almost formed a complete circle separating the inner center from the outer rain bands.

During the weakening of the TY center, similar cloud band formed on northern Luzon and shifted northward, as the MTSAT observation, is simulated (Figs. 6a - d). The simulated echo over the ocean west of Luzon (Area A) also developed from 06 UTC to 18 UTC 18. An area of higher dBz expanded northward to Area A at 12 UTC 18 (Fig. 6d). As the echo over northern Luzon also intensified and extended southeastward, the higher dBz area from north connects with the higher dBz area extending from Central Luzon, a ring shape of high reflectivity formed albeit barely visible from Fig. 6d. Later at 18 UTC 18 (Fig. 6e), the higher dBz area over Northern Luzon moved northward to the coastal area and connected with the higher dBz area over the ocean west of Luzon, where the echoes condensed to a narrower and more intensive one. This higher dBz band extended further downstream to the ZMR. Based on the TWRF modeling results, Fig. 7 illustrates that the enhancement of the rain band echo is related to the moisture flux convergence of the entire layer of the atmosphere. Moisture flux convergence (MFC) formed in the western side of Luzon at 06 UTC 18.

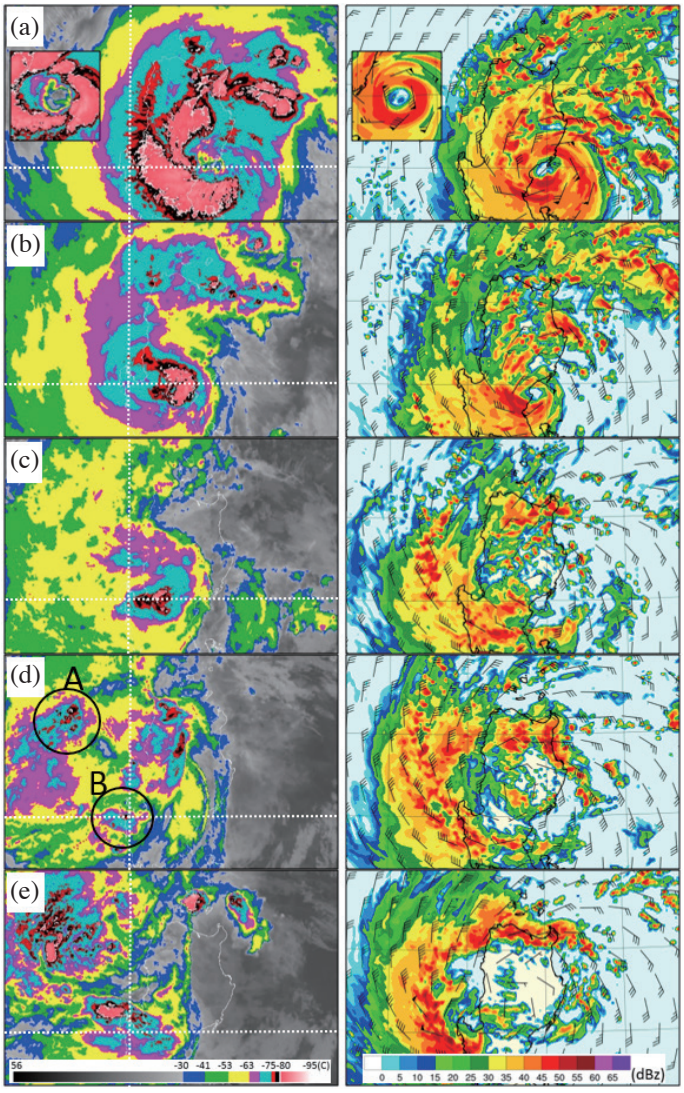

Fig. 6. The MTSAT infrared cloud images (left panel, °C, scale in bottom) and TWRF predicted (right panel) 10 m winds (a bar for 10 knots, a flag for 50 knots) and radar maximum reflectivity (dBz, scale in bottom) at (a) 18 UTC 17, (b) 00 UTC 18, (c) 06 UTC 18, (d) 12 UTC 18, and (e) 18 UTC 18 October. The cloud image and the TWRF predicted fields near TY center at 12 UTC 17 are in the insets of (a), respectively. The dashed lines in the diagrams of left panel indicate 18°N and 120°E. Circles in (d) define Areas A and B.

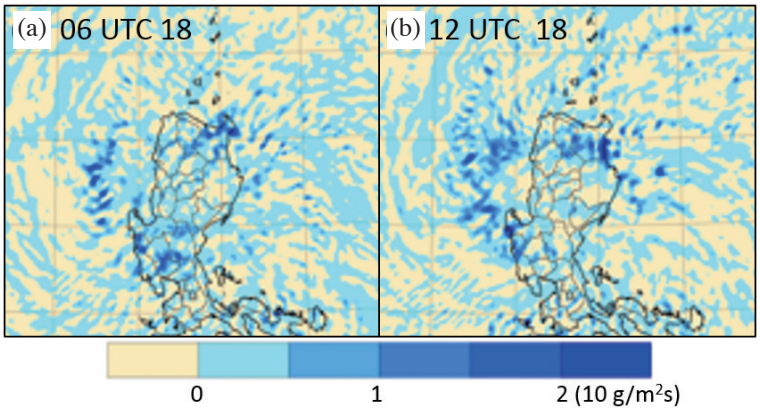

Fig. 7. Moisture flux convergence (in units of 10 g m^{-2} s^{-1}, scale in bottom) predicted by the TWRF model for (a) 06 UTC and (b) 12 UTC 18 October.

The MFC increased and expanded northward, connecting with the MFC belt in Northern Luzon. The MFC also extended southward to reach the ZMR at 12 UTC 18. Under this circumstance of reforming the outer rain band of TY Koppu as one connected system, the accumulated 3-hour rainfall increased and reached the first peak of the intensive rain at the selected location (Fig. 5).

The intensive rain at Baguio is probably due to the same mechanism of the TWRF-predicted rainfall at the selected location in the ZMR. The weakened TY gradually reformed a rain band in the open sea located west of Luzon, and the rain band, as well as the cyclonic circular flow, gradually concentrated and intensified to reorganize as a strong circular rain band when the TY center moved westward across Luzon. One difference between the TWRF-simulated radar echoes and the MTSAT image (Fig. 6) is the timing of the stronger dBz reformed in Western Luzon is earlier than that of the cloud development observed from MTSAT. A stronger dBz in ZMR is found at 12 UTC 18 when the MTSAT CTT (Fig. 6d) near the ZMR reached the warmest. Given that the TWRF-predicted time of the maximum rainfall and the high reflectivity echo at the selected location are earlier than that of the actual rainfall at Baguio, additional MTSAT images are prepared in Fig. 8 to investigate the evolution of the observed rainfall further. The figure shows similar consociation and intensification of the system from 18 UTC 18 to 03 UTC 19. The lower CTT area in Area A at 18 UTC 18 (Fig. 6e) moved closer to Area B at 21 UTC 18. These two lower CTT areas combined at 00 UTC 19 and intensified in west of Baguio at 03 UTC 19. Later, the system weakened gradually from 03 UTC to 09 UTC 19 before the system regained intensity at 12 UTC 19. The timing of the consociation of the system, as well as the intensification and weakening of the system observed from MTSAT, consists of the time of the rainfall variation observed in Baguio (Fig. 5). The rainfall that peaked at 03 UTC 19 agrees with the intensity reaching the maximum around 00 UTC to 03 UTC 19. The rain that broke at 09 UTC 19 also agrees well with the system weakening from 06 to 09 UTC 19 and redeveloping at 12 UTC. The satellite observation validates the TWRF simulation results, which show that the reorganization process of TY Koppu over the ocean caused the intensive rainfall at Baguio. A similar formation of the rain band or reorganization of the eyewall has been documented for TYs encountered Taiwan. Huang et al. (2016) reported that an unusual double intense rainfall

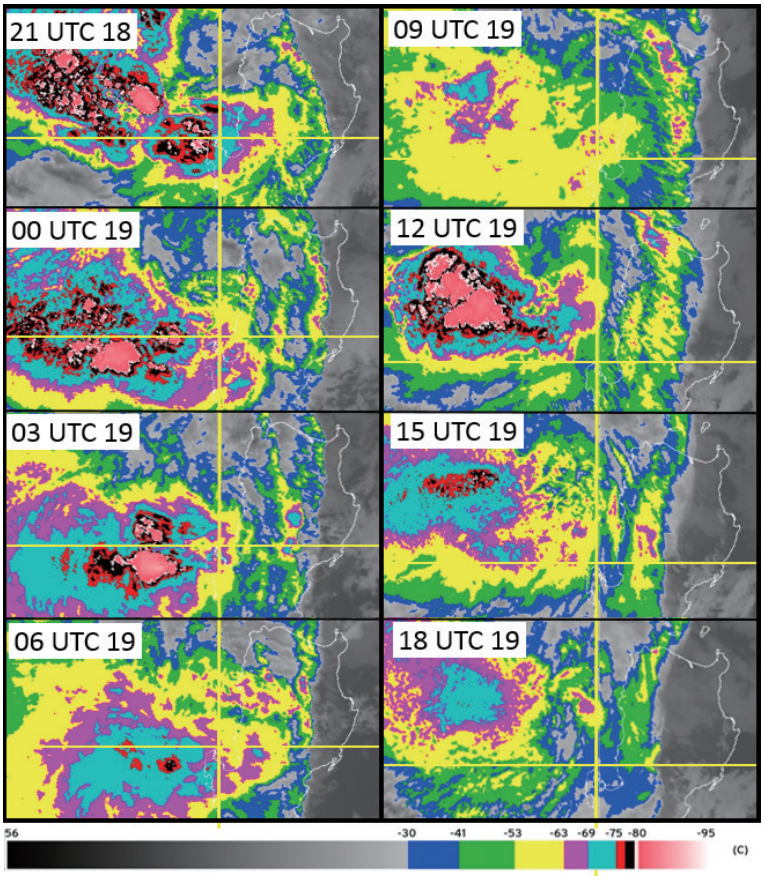

Fig. 8. Three-hour MTSAT infrared cloud top temperature (°C, scale in bottom) imagery from 21 UTC 18 to 21 UTC 19 October (top down, left to right). Coastline of Northern Luzon is outlined. 120°E and the latitude of Baguio are shown in yellow lines.

peak was found in southern Taiwan when TY Fanapi encountered Taiwan from the east in year 2000, with a peak of 1127 mm (in 61 hours) over the mountain range and the other (946 mm) near the coastal area. By analyzing the radar observations, Liou et al. (2016) concluded that TY Fanapi's eye and eyewall disappeared on the eastern side of Taiwan's Central Mountain Range (CMR) after Fanapi made landfall but re-emerged on the western side of the CMR, and the reorganization of the eyewall caused intensive rainfall in the coastal area. In contrast to the reorganization of TY Koppu, that of TY Fanapi had much heavier rainfall, no few hours of break during the intensive rainfall period, and the duration of the eyewall was much shorter.

4.2 Structural Change

The TWRF-predicted relative humidity, geopotential height (GPH), and winds at 500 and 700 hPa are presented in Fig. 9. The figure shows the center of TY Koppu at 500 hPa moved westward before 30 h of prediction. The GPH low centers and the wind circulation centers were able to maintain co-located before 18 h of prediction (valid at 06 UTC 18) even through Koppu weakened considerably and the center at lower level moved slower after the TY moving over land. Later, the GPH center no longer co-located with wind center and the center at upper level also not vertically-aligned with the center underneath. The center displacement became largest and the intensity of Koppu reached the weakest at 24 h (12 UTC 18). The system regained the intensity and the centers located closer at 30 h before the system moving northward to the bay with intensity further intensified at 36 h (00 UTC 19). More complicated structural change showed at the 925 hPa surface (Fig. 10). At 12 hours of prediction (00 UTC 18), the center location at

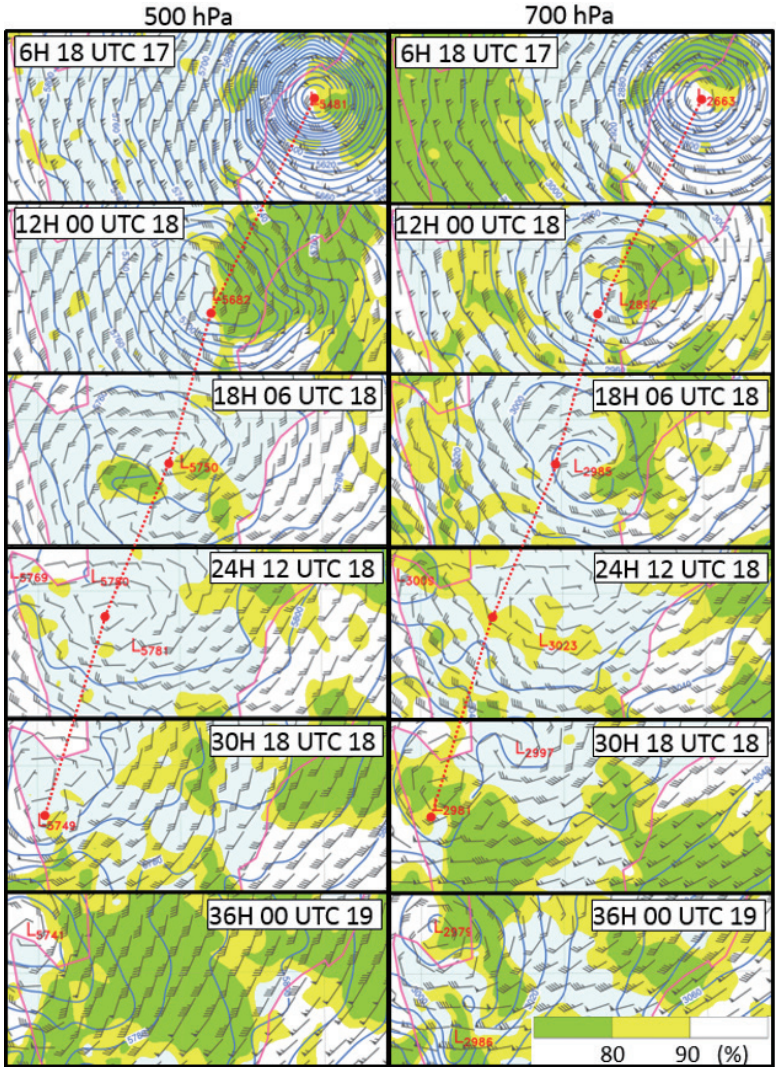

Fig. 9. Relative humidity (%, color scale in bottom), geopotential height (contours, in m) and the wind bars (in kts) at 500 (left) and 700 hPa (right) from the TWRF prediction at 6, 12, 18, 24, 30, and 36 hours. Coastline of Northern Luzon is outlined (domain shifted northward at 36 hours). Center at 500 hPa is denoted in red (not at 36 hours).

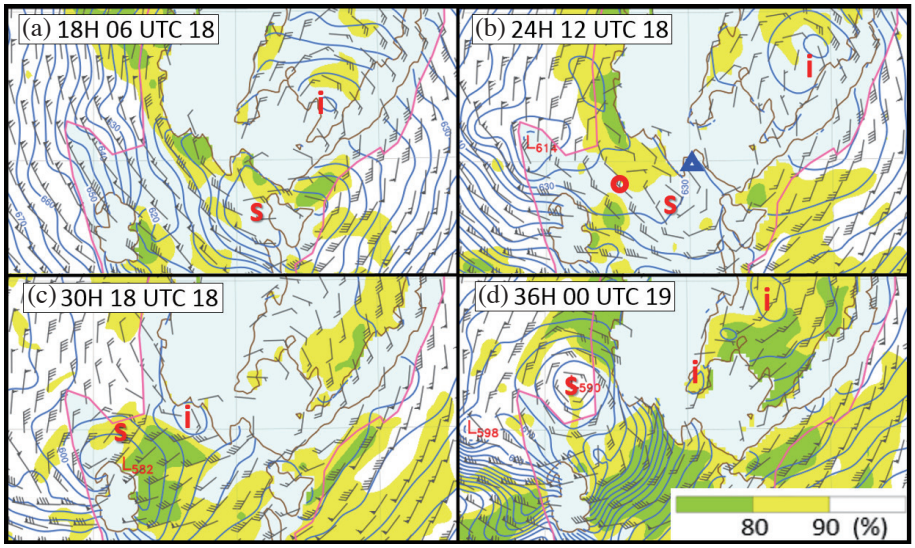

Fig. 10. Similar to Fig. 9: relative humidity, geopotential height and wind bars at 925 hPa from the TWRF prediction at (a) 18, (b) 24, (c) 30, and (d) 36 hours. Symbols s and i denote the center and the induced center location, respectively. Symbols circle and triangle in (b) indicate the center location at 500 and 700 hPa, respectively.

925 hPa (figure not shown) was roughly the same as that of at 700 hPa, and those were at the low-lying area between mountains and were in east of the center at 500 hPa. It looked like the lower level center was blocked and centers were tilted to the west along height due to the terrain effect. Six hours later (06 UTC 18), the center moved to the west of the mountain range (Fig. 10a). The trough in lee side of the SMR intensified with an induced low center. By the time of the system moved further inland at 12 UTC 18 (Fig. 10b), although the TY circulation center was still able to be maintained, however no GPH center co-located and the stronger winds were predicted in the outer ring away from the circulation center. The intensity significant weakened and the separation of the centers among different levels was clearly shown. Meanwhile, the terrain induced center on lee side of SMR expanded in size and moved northward in Cagayan Valley with cyclonical circulation associated. Another GPH low center formed near Bolinao. Where, strong northeasterly winds upstream of the GPH low and strong northwesterly winds downstream of the GPH low induced strong moisture convergence (Fig. 7b), high radar reflectivity (Fig. 6d), and intensive rainfall (Fig. 5). This GPH low also extended upward to 500 hPa (Fig. 9). The low center near Bolinao was probably formed partially by the diabatic effect of latent heating. In north of Bolinao, northerly winds were from the dry area lee side of the COMR. The southward advection of the dry air contributed to the southward shifting of the rain band (showed in right panel of Figs. 6d and e) and the decreasing of the rainfall at the selected location after it reaching to the first peak of the rainfall at 15UTC 18 (Fig. 5). A note is that the moist air from ocean was able to reach to the central area of the TY through the lower-lying valley between the mountain ranges at 12 UTC 18. Three hours later (figures not showed), the 925 hPa GPH center intensified and aligned with centers at other level. The better vertically aligned, mass and flow co-located center became the core of TY Koppu after the reorganization process.

The flow confluence zone shifted further to the south when the system moved closer to the coastline at 18 UTC 18 (Fig. 10c). Terrain effect now occurred strongly from the ZMR. A lee side low and dry area was predicted on the eastside of ZMR. An induced low and weak cyclonic flow center was found in south of the COMR. After the TY moved northward into the bay six hours later at 00 UTC 19 (Figs. 9 and 10d), center was better vertically aligned mass and flow co-located. Although the core region was away from the directly influence of the ZMR, but was still under the effect of the COMR and CBMR. Dry air in the lee side of the mountain north of the TY center not only limited at the lower level but also extended to the deeper layer (Fig. 9). At 42 h of prediction (06 UTC 19, Fig. 11), when the system moved further to the north, strong terrain effect were again clearly notable from the figure. Centers were not vertically aligned, mass center and flow center were not co-located. Dry area and trough on lee side of COMR expanded, and the wind speed near the center were significantly reduced. Another low with the cyclonic circulation center also formed over the Cagayan Valley. The low-level flow convergence zone at 925 hPa shifted northward and the distribution of the flow near the convergence zone resembled to that of at 12 UTC 18 (Fig. 10b). The approaching of the flow convergence zone increased the rainfall at the selected location (Fig. 5). Later at 48 h of prediction (12 UTC 19, figure not shown), the convergence zone passed

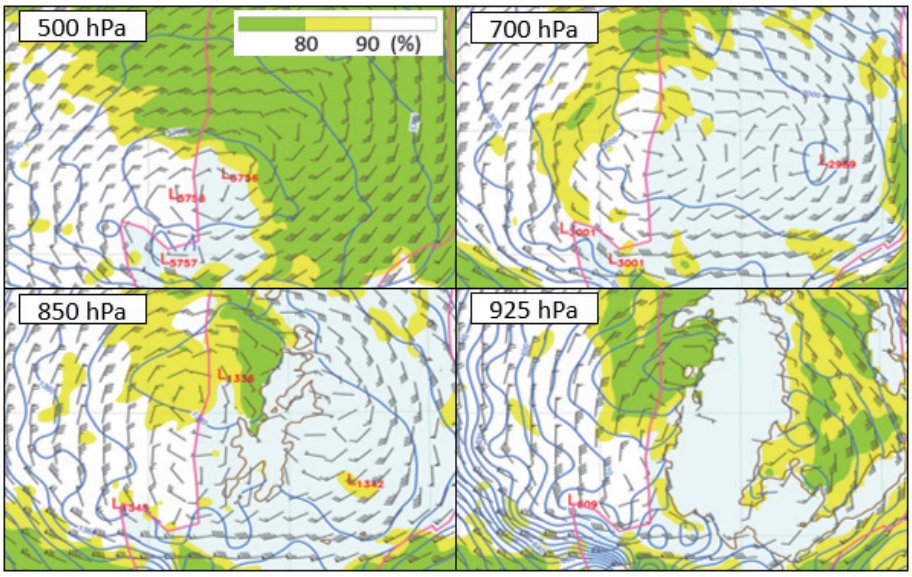

Fig. 11. Similar to Fig. 9: relative humidity, geopotential height and wind bars at 500, 700, 850, and 925 hPa from the TWRF 42 hours of prediction (valid 06 UTC 19 October).

the selected location. The approaching and the passing of the convergence zone consisted with the rainfall reaching to the second peak at 06 UTC 19 shown in Fig. 5. At 60 and 72 h of prediction (figures not shown), the system remained under the mountainous terrain influence and did not organize as a normal TC. Strong winds were in some distance away from the center. The system/rainfall is stronger/larger than the observation in the later stage of the TWRF prediction (Fig. 4) probably due to the overestimation of the winds in the outer ring. As the southern lateral boundary of the fine-resolution grids is close to the TY track, whether the overestimation of the winds related to the domain setup still waiting for more investigations.

4.3 Terrain Effect

A sensitivity simulation with the terrain height of the Luzon Island set to 0 km (hereafter noted as TH0) was conducted to study the effect of terrain on the movement and rainfall of TY Koppu. Figure 12a shows a similar center recurve to the north in TH0 as in the prediction with normal terrain height (hereafter noted as CTR). However, the track in TH0 is to the right-hand side of that in CTR. Without high terrain, no low-humidity air was locked in the lee side of the high terrain. The core of Koppu was able to move directly over Northern Luzon and to maintain, basically, in vertical aligned and the mass and wind fields co-located (example as in Figs. 12b and c) to passing over the area without the SMR and COMR. Similar track deflection was reported by Yeh and Elsberry (1993). Their model simulations showed the southward (left hand side) drift of a westward slow-moving intensive vortex to encounter the southern portion of a barrier. As for the rainfall, Fig. 12d shows that the rainfall in TH0 is more concentrated in the core region. The heavy rainfall on the windward side of the high mountain ranges in CTR no longer existed in TH0. For example, rain of more than 300 mm is reduced to less than 150 mm on east slope of SMR at 00 - 12 h of prediction. More intensive and more condensed rain bands were found in CTR at a later period (36 and 48 h) of the simulation. However, both of the rainfall in TH0 and in CTR were heavier on the southern side of the center. Even without the high terrain, an outer rain band was also found near Bolinao during 12 - 24 hours of TH0 simulation, when the core center was still located in Eastern Luzon. These two environmental conditions provide a favorable background to the formation of the intensive rain band over Western Luzon when Koppu made landfall at the Philippines. The strong northerly monsoon on the west side of Luzon (right panel of Fig. 6) which can be helpful for providing the favorable background.

5. SUMMARY AND CONCLUDING REMARKS

The Philippines is an area most affected by tropical cyclones (TCs). However, literature on the rainfall and structural changes of TCs in the area is limited. Typhoon (TY) Koppu made landfall at the Philippines in 2015. Intense rainfall of 775.4 mm in 24 h was observed at Baguio, and the rainfall is unique in its small horizontal scale and its double peaks in the three-hourly rainfall sequence. This study used the TWRF model (Hsiao et al. 2020) of the Central Weather Bureau (CWB), Taiwan to improve the understanding of the rainfall characteristics and structural changes of TY Koppu encountering the mountainous

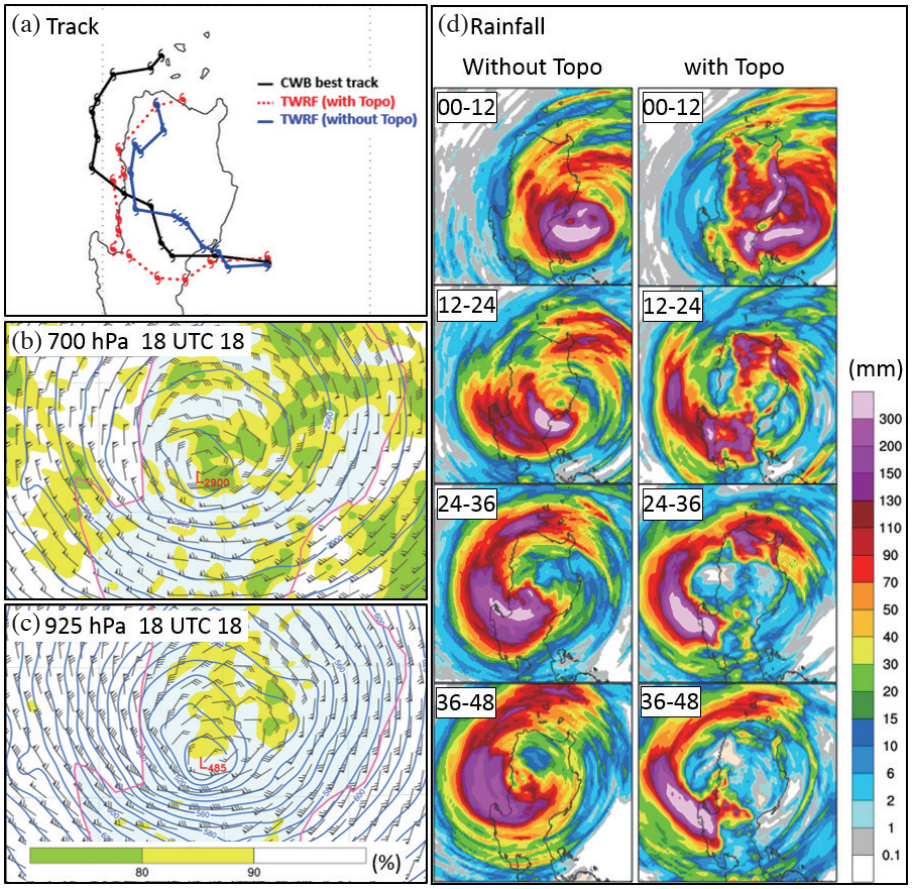

Fig. 12. TWRF simulated result of Typhoon Koppu without high terrain (without Topo). (a) Track, (b) and (c) relative humidity, geopotential height and wind bars (units same as in Fig. 9) at 700 and 925 hPa, respectively, for 18 UTC 18 October (30 hours of simulation), and (d) 12-hour accumulated rainfall for 00 - 12, 12 - 24, 24 - 36, and 36 - 48 hours of simulation (from top down). For facilitating comparison, the track and the 12-hour accumulated rainfalls of TWRF prediction with normal terrain (with Topo) are added in (a) and (d), respectively.

terrain. The observation data, initial fields, and model lateral boundary condition fields were collected in real-time at 1200 UTC 17 October. The 12-hour accumulated surface station-observed rainfall and the analyzed rainfall by the NOAA CPC using the morphing technique (CMORPH, Joyce et al. 2004) were also discussed.

Verifying the CWB, JMA, JTWC, and PAGASA best tracks, the largest TWRF-predicted track error within 72 hours of prediction is 145 km that occurred at 60 hours of prediction. Similar rainfall distribution in Luzon, similar rainfall shifting to the north in the western part of Northern Luzon, and similar rainfall sequence at Baguio could also be predicted by TWRF, except that the location of the maximum rainfall was predicted to the south, and the starting time of intensive rainfall was predicted earlier than that of the observation. A comparison among the CMORPH-analyzed rainfall, surface-observed rainfall, and TWRF-predicted rainfall shows that the CMORPH rainfall reflected the general rainfall feature of synoptic weather; however, it considerably underestimated the later stage rainfall of TY Koppu over Western Luzon.

The modeling results showed that the high terrain in Luzon played an important role to affect the structure, intensity and the movement of TY Koppu. High terrain blocked or deflected the impending flow, ridges formed over the windward side of the mountains, and troughs or even secondary lows formed over the lee side of the mountains. Through verification against satellite infrared imagery, the modeling results also showed that the outer rain band of TY Koppu caused the heavy rainfall. The rain band gradually reorganized over the nearby ocean and coastal area west of Luzon as Koppu weakened after it encountered with high mountain ranges. The results further showed that the terrain located south of the center enhanced the rainfall of the rain band. However, the mountains in the north of the center played a role in weakening the band; as the dryer air intruded the system after passing over the mountains. Strong northerly winds of the dryer air also contributed to push the band southward. The formation and intensification, as well as the weakening and southward shifting of the rain band, induced the first phase of the increasing and decreasing of the 3-hour accumulated rainfall at Baguio.

The rain band then moved northward again as TY Koppu moved northward. The approaching and passing of the rain band contributed to the second phase of the unique intensive rainfall at Baguio.

The TWRF modeling results suggested the low-lying valley between the Cordillera Mountain Range and the Zambales Mountain Range seems providing a channel for the moist air to be supplied into the TY center. The moist air helps Koppu to maintain or even to enhance its intensity. Moreover, the unique U-shaped high terrain in Northern Luzon looks like favorable for the secondary low or circulation center to be formed over the Cagayan Valley. Further studies are needed to understand their impact on the movement and the rainfall distribution of TY Koppu. A limitation of this study is that the observation in the Luzon area is somewhat insufficient to show detailed rainfall, wind, and pressure distributions. Adding a few stations in some critical locations that cooperate with weather radars will greatly reduce uncertainty on the analysis of the track and structure of approaching TCs.

Acknowledgements This study is supported by the Ministry of Science and Technology, Taiwan, R.O.C. under grant MOST 105-2625-M-052-004 and by the VOTE Program under Ministry of Science and Technology, Taiwan and Department Of Science and Technology, Philippines. Comments/suggestions made by two reviewers are helpful to improve the presentation of this paper. The authors would also like to thank Mr. Chun-Teng Cheng for his constructive work in Koppu simulation with TWRF.

REFERENCES

Brand, S. and J. W. Blelloch, 1973: Changes in the characteristics of typhoons crossing the Philippines. *J. Appl. Meteorol. Climatol.*, **12**, 104-109, doi: 10.1175/1520-0450(1973)012<0104:CITCOT>2.0.CO;2. [Link]

Brand, S. and J. W. Blelloch, 1974: Changes in the characteristics of typhoons crossing the island of Taiwan. *Mon. Weather Rev.*, **102**, 708-713, doi: 10.1175/1520-0493(1974)102<0708:CITCOT>2.0.CO;2. [Link]

Cayanan, E. O., T.-C. Chen, J. C. Argete, M.-C. Yen, and P. D. Nilo, 2011: The effect of tropical cyclones on southwest monsoon rainfall in the Philippines. *J. Meteorol. Soc. Jpn.*, **89A**, 123-139, doi: 10.2151/jmsj.2011-A08. [Link]

Chen, Y.-H., H.-C. Kuo, C.-C. Wang, and Y.-T. Yang, 2017: Influence of southwest monsoon flow and typhoon track on Taiwan rainfall during the exit phase: Modelling study of typhoon *Morakot* (2009). *Q. J. R. Meteorol. Soc.*, **143**, 3014-3024, doi: 10.1002/qj.3156. [Link]

Chien, F.-C. and H.-C. Kuo, 2011: On the extreme rainfall of Typhoon Morakot (2009). *J. Geophys. Res.*, **116**, D05104, doi: 10.1029/2010jd015092. [Link]

Chou, K.-H., C.-C. Wu, and Y. Wang, 2011: Eyewall evolution of typhoons crossing the Philippines and Taiwan: An observational study. *Terr. Atmos. Ocean. Sci.*, **22**, 535-548, doi: 10.3319/TAO.2011.05.10.01(TM). [Link]

Cinco, T. A., R. G. de Guzman, A. M. D. Ortiz, R. J. P. Delfino, R. D. Lasco, F. D. Hilario, E. L. Juanillo, R. Barba, and E. D. Ares, 2016: Observed trends and impacts of tropical cyclones in the Philippines. *Int. J. Climatol.*, **36**, 4638-4650, doi: 10.1002/joc.4659. [Link]

Hong, J.-S., C.-T. Fong, L.-F. Hsiao, Y.-C. Yu, and C.-Y. Tzeng, 2015: Ensemble Typhoon Quantitative Precipitation Forecasts Model in Taiwan. *Weather Forecast.*, **30**, 217-237, doi: 10.1175/waf-d-14-00037.1. [Link]

Hsiao, L.-F., C.-S. Liou, T.-C. Yeh, Y.-R. Guo, D.-S. Chen, K.-N. Huang, C.-T. Terng, and J.-H. Chen, 2010: A vortex relocation scheme for tropical cyclone initialization in Advanced Research WRF. *Mon. Weather Rev.*, **138**, 3298-3315, doi: 10.1175/2010mwr3275.1. [Link]

Hsiao, L.-F., D.-S. Chen, J.-S. Hong, T.-C. Yeh, and C.-T. Fong, 2020: Improvement of the numerical tropical cyclone prediction system at the Central Weather Bureau of Taiwan: TWRF (Typhoon WRF). *Atmosphere*, **11**, 657, doi: 10.3390/atmos11060657. [Link]

Hsu, Y. C., 1960: The problems of typhoon forecasting over Taiwan and its vicinity. Proc. U. S. Asian Military Weather Sympos.

Huang, C.-Y., Y.-H. Kuo, S.-H. Chen, and F. Vandenberghe, 2005: Improvements in typhoon forecasts with assimilated GPS occultation refractivity. *Weather Forecast.*, **20**, 931-953, doi: 10.1175/waf874.1. [Link]

Huang, C.-Y., I.-H. Wu, and L. Feng, 2016: A numerical investigation of the convective systems in the vicinity of southern Taiwan associated with Typhoon Fanapi (2010): Formation mechanism of double rainfall peaks. *J. Geophys. Res.*, **121**, 12647-12676, doi: 10.1002/2016jd025589. [Link]

Joyce, R. J., J. E. Janowiak, P. A. Arkin, and P. Xie, 2004: CMORPH: A method that produces global precipitation estimates from passive microwave and infrared data at high spatial and temporal resolution. *J. Hydrometeorol.*, **5**, 487-503, doi: 10.1175/1525-7541(2004)005<0487:CAMTPG>2.0.CO;2. [Link]

Lee, C.-S., Y.-C. Liu, and F.-C. Chien, 2008: The secondary low and heavy rainfall associated with Typhoon Mindulle (2004). *Mon. Weather Rev.*, **136**, 1260-1283, doi: 10.1175/2007mwr2069.1. [Link]

Lee, W.-C., B. J.-D. Jou, P.-L. Chang, and F. D. Marks Jr., 2000: Tropical cyclone kinematic structure

retrieved from single-Doppler radar observations. Part III: Evolution and structures of Typhoon Alex (1987). *Mon. Weather Rev.*, **128**, 3982-4001, doi: 10.1175/1520-0493(2000)129<3982:TCKSRF>2.0.CO;2. [Link]

Li, P. C., 1963: Terrain effects on typhoons approaching Taiwan. Proc. U. S. Asian Military Weather Sympos.

Lin, S.-J. and K.-H. Chou, 2018: Characteristics of size change of tropical cyclones traversing the Philippines. *Mon. Weather Rev.*, **146**, 2891-2911, doi: 10.1175/MWR-D-18-0004.1. [Link]

Lin, Y.-L., S.-Y. Chen, C. M. Hill, and C.-Y. Huang, 2005: Control parameters for the influence of a mesoscale mountain range on cyclone track continuity and deflection. *J. Atmos. Sci.*, **62**, 1849-1866, doi: 10.1175/jas3439.1. [Link]

Liou, Y.-C., T.-C. C. Wang, and P.-Y. Huang, 2016: The inland eyewall reintensification of Typhoon Fanapi (2010) documented from an observational perspective using multiple-Doppler radar and surface measurements. *Mon. Weather Rev.*, **144**, 241-261, doi: 10.1175/MWR-D-15-0136.1. [Link]

Liu, G.-R., T.-H. Kuo, P.-Y. Leu, T.-H. Lin, and C.-C. Liu, 2001: An estimation of typhoon intensity and the prediction of its track by using MSU data. *Terr. Atmos. Ocean. Sci.*, **12**, 615-634, doi: 10.3319/TAO.2001.12.4.615(A). [Link]

Skamarock, W. C., J. B. Klemp, J. Dudhia, D. O. Gill, D. Barker, M. G. Duda, X. Huang, W. Wang, and J. G. Powers, 2008: A description of the Advanced Research WRF version 3. No. NCAR/TN-475+STR, NCAR Technical Note, University Corporation for Atmospheric Research, 113 pp, doi: 10.5065/D68S4MVH. [Link]

Wang, C.-C., Y.-H. Chen, H.-C. Kuo, and S.-Y. Huang, 2013: Sensitivity of typhoon track to asymmetric latent heating/rainfall induced by Taiwan topography: A numerical study of Typhoon Fanapi (2010). *J. Geophys. Res.*, **118**, 3292-3308, doi: 10.1002/jgrd.50351. [Link]

Wang, S.-T., 1980: Prediction of the behavior and strength of typhoons in Taiwan and its vicinity. Research Report No. 018., National Science Council Research, Taipei, Taiwan, 100 pp.

Wu, C.-C. and Y.-H. Kuo, 1999: Typhoons affecting Taiwan: Current understanding and future challenges. *Bull. Amer. Meteorol. Soc.*, **80**, 67-80, doi: 10.1175/1520-0477(1999)080<0067:TATCUA>2.0.CO;2. [Link]

Wu, C.-C., K.-H. Chou, H.-J. Cheng, and Y. Wang, 2003: Eyewall contraction, breakdown and reformation in a landfalling typhoon. *Geophys. Res. Lett.*, **30**, 1887, doi: 10.1029/2003GL017653. [Link]

Wu, C.-C., K.-H. Chou, P.-H. Lin, S. D. Aberson, M. S. Peng, and T. Nakazawa, 2007: The impact of dropwindsonde data on typhoon track forecasts in DOTSTAR. *Weather Forecast.*, **22**, 1157-1176, doi: 10.1175/2007WAF2006062.1. [Link]

Yang, M.-J., Y.-C. Wu, and Y.-C. Liou, 2018: The study of inland eyewall reformation of Typhoon Fanapi (2010) using numerical experiments and vorticity budget analysis. *J. Geophys. Res.*, **123**, 9604-9623, doi: 10.1029/2018jd028281. [Link]

Yeh, T.-C. and R. L. Elsberry, 1993: Interaction of typhoons with the Taiwan orography. Part I: Upstream track deflections. *Mon. Weather Rev.*, **121**, 3193-3212, doi: 10.1175/1520-0493(1993)121<3193:IOTWTT>2.0.CO;2. [Link]